Structural Study of the Lipid-Containing Bacteriophage PRD1 and Its Capsid and DNA Components by Laser Raman Spectroscopy†

Dennis H. Bamford,‡ Jaana K. H. Bamford,‡ Stacy A. Towse,§ and George J. Thomas, Jr.*,§

Department of Genetics, University of Helsinki, Helsinki SF-00100, Finland, and Division of Cell Biology and Biophysics, University of Missouri—Kansas City, Kansas City, Missouri 64110-2499

Received January 24, 1990; Revised Manuscript Received March 23, 1990

ABSTRACT: The Raman spectrum of a virus contains the structural signature of each of its molecular components (Thomas, 1987). We report the first Raman spectrum obtained from an intact, lipid-containing virus—the icosahedral bacteriophage PRD1—and show that this spectrum contains characteristic structure markers for the major capsid protein, the packaged double-stranded DNA genome, and the viral membrane which resides between the capsid and DNA. We find that the packaged genome of PRD1 exhibits Raman markers typical of the B-DNA secondary structure. Comparison of the Raman spectrum of the packaged DNA with that of protein-free DNA extracted from the virion shows further that the B-form secondary structure is not significantly perturbed by packaging in the virion. The Raman signature of the PRD1 membrane, monitored within the virion at 4 °C, is that of a phospholipid liquid-crystalline phase. The PRD1 capsid, which comprises several hundred copies of the major coat protein P3 (product of viral gene III) and a few copies of minor proteins, incorporates P3 capsomers predominantly in the β-sheet conformation. The β-sheet structure of P3 is maintained in the fully assembled PRD1 virion, as well as in the empty capsid. The present results demonstrate the feasibility of obtaining structural information from the three different classes of biomolecules—nucleic acid, protein, and lipid—which constitute a membrane-lined virus particle. Our results also demonstrate that the coat protein and double-stranded DNA components of a lipid-containing bacteriophage share many structural features in common with bacteriophage lacking a lipid membrane.

Recent progress in the study of membrane organization and function makes it increasingly clear that mechanisms of membrane biosynthesis, protein insertion, and protein translocation are universal phenomena which occur with many similarities in both eukaryotic and prokaryotic organisms (Saier et al., 1989). Accordingly, the bacterial membrane provides an effective model for investigating many membrane-related processes of higher organisms. Similarly, bacteriophages with structural membranes provide powerful model systems for elucidating membrane organization and probing the genetic control of membrane assembly and translocation processes (Mindich & Bamford, 1988).

Bacteriophage PRD1 is a member of the family of double-stranded (ds) DNA viruses capable of infecting Gram-negative bacterial cells harboring a plasmid of the P, N, or W compatibility group. Among the hosts are *Escherichia coli* and *Salmonella typhimurium* (Olsen et al., 1974; Bamford et al., 1981; Savilahti & Bamford, 1986). The coat of the icosahedral virion is composed of a major protein, P3 (43.1 kDa), and a minor protein, P5 (34.3 kDa), encoded respectively by viral genes III and V (Bamford & Mindich, 1982; Bamford & Bamford, 1990). The viral membrane, located inside the protein coat, is composed of lipids and at least 15 distinct protein species (Bamford & Mindich, 1982). The dsDNA genome, which is packaged within the membrane vesicle, is a linear molecule of approximately 14700 base pairs (McGraw et al., 1983). As in the cases of adenovirus (Tamanoi, 1986) and bacteriophage ϕ29 (Salas, 1988), a protein which primes DNA replication is covalently linked to the 5′ terminus of each strand of PRD1 DNA (Bamford & Mindich, 1984).

The PRD1 virion, like other members of its class, is composed by weight of approximately 15% lipid, 15% DNA, and 70% protein (Wong & Bryan, 1978; Davis et al., 1982). The phospholipid composition of the virus membrane can be altered drastically by growing the virus in mutants of *E. coli* which are defective in either fatty acid or phospholipid metabolism (Muller & Cronan, 1983). In the genome of the related phage PR4, the mole percent GC is 46 (Davis et al., 1982). Preliminary sequencing of 95% of the PRD1 genome indicates that the base composition is 48% GC (D. H. Bamford and J. K. H. Bamford, unpublished results). The major capsid protein of PR4 can be specifically cross-linked to phosphatidylglycerol, and it has been suggested on this basis that the capsid protein or its capsomer complex is embedded in a phosphatidylglycerol annulus (Davis & Cronan, 1985).

Use of nonsense phage mutants (Mindich et al., 1982a; Davis & Cronan, 1983) to investigate morphogenesis has led to an assembly model in which the capsomers are involved in pinching off a phage-specific vesicle from the host plasma membrane (Mindich & Bamford, 1988). The empty capsid subsequently packages dsDNA. The role of the capsomer in this process is viewed as analogous to that of clathrin for endocytosis in eukaryotic cells. A more comprehensive review of recent results on the PRD1 assembly pathway has been given recently (Mindich & Bamford, 1988). These genetic and biochemical studies have made it possible to isolate and purify in milligram quantities defined viral precursor particles in addition to the infective virion (Mindich et al., 1982a,b; Bamford & Mindich 1982; Bamford & Bamford, 1990).

To further understand the steps involved in the pathway of PRD1 morphogenesis, it is necessary to obtain more detailed structural information about the mature PRD1 virion, its precursor particles, and their macromolecular constituents. In this investigation, we demonstrate the feasibility of laser Raman spectroscopy for structural assessment of PRD1 and its subassemblies. Our results show conformational features

†Supported by the National Institutes of Health (Grant AI11855) and the Academy of Finland. This is part 33 in the series Studies of Virus Structure by Laser Raman Spectroscopy from the U.S. laboratory.

*To whom correspondence should be addressed.

‡University of Helsinki.

§University of Missouri—Kansas City.

0006-2960/90/0429-5982$02.50/0

of the protein, DNA, and lipid components of PRD1 and permit conclusions to be reached about the packaging of dsDNA in a membrane-lined protein shell.

Previous applications of Raman spectroscopy in structural studies of viruses have been limited to nonenveloped bacteriophages and plant viruses, i.e., virions composed only of protein and nucleic acid. The earlier work has been reviewed recently (Thomas, 1987). Typically, the Raman scattering spectrum of a virus contains many bands from each type of viral molecular component. Each band arises from the transfer of discrete units of energy from a beam of electromagnetic radiation (laser) to the scattering molecules in the form of vibrational energy (frequency). The selection rules governing such transfers are well-known, and the spectral frequencies and intensities thus serve as a rich molecular fingerprint (Thomas & Kyogoku, 1977; Carey, 1982). The assignment of each of the Raman bands in the spectrum of a virus to a particular molecular component, and where possible to vibrations of specific chemical groups of the molecular component, is facilitated by model compound studies and serves as the basis for use of the Raman spectrum to diagnose biomolecular structure (Thomas, 1987). Extensive studies have been made of the conformation dependence of both the frequencies and intensities of Raman bands for all classes of biomolecules (Spiro, 1987). Comprehensive reviews for proteins (Tu, 1986), nucleic acids (Thomas & Wang, 1988), and lipids (Lord & Mendelsohn, 1981; Levin, 1984) have been given.

Experimental Procedures

Preparation of Virus and Viral Components. Wild-type PRD1 was grown on *Salmonella typhimurium* LT2 DS88 (Bamford & Bamford, 1990), using Luria–Bertani broth (Maniatis et al., 1982), concentrated with poly(ethylene glycol) 6000, and purified by rate zonal centrifugation in a Sorvall AH 627 rotor. The virus band was collected, and the particles were pelleted by differential centrifugation and resuspended in buffer C (1 mM $MgCl_2$/10 mM Tris-HCl, pH 7.4) as described (Bamford & Bamford, 1990). This virus preparation, designated 1× purified, contained 1.7×10^{13} pfu/mL and a protein concentration of 1.5 mg/mL as assayed with a BSA standard (Bradford, 1976). To further separate empty particles from the virus, the rate zonal and pelleting steps were repeated, and the final pellet was resuspended in buffer C on ice. This preparation, designated 2× purified, yielded a titer of 2.5×10^{13} pfu/mL and a protein concentration of 2.3 mg/mL. The 1× and 2× preparations were kept on ice until analyzed by Raman spectroscopy.

Protein capsomers were isolated from the virus by treatment with 2 M guanidine hydrochloride, followed by incubation for 5 min at room temperature and ultracentrifugation in the Beckman Airfuge (A-95 rotor, 4 °C, 30 psi, 30 min) to sediment membrane and DNA components. Major and minor capsid proteins in the supernatant were separated in a 10–40% weight/volume sucrose gradient (SW41 rotor, 28 h, 35 000 rpm, 10 °C). After fractionation, the proteins were assayed by denaturing gel electrophoresis (SDS–PAGE). Fractions containing the major capsomer were pooled and dialyzed against buffer C at 4 °C. The purity of the dialyzed fraction was confirmed by SDS–PAGE and ethidium bromide fluorescence. No proteins other than P3 and no DNA were detected. In a typical P3 preparation, 3.0 mL of 1× virus preparation yielded about 2.5 mg of P3. The P3 isolate was maintained in the cold (4 °C) in buffer C at 0.1 mg/mL until further concentrated for Raman spectroscopy. Additional details of the capsomer preparation procedure have been described (Bamford & Bamford, 1990).

Virus particles (1× purified), which were obtained from a 1.5-L lysate, were resuspended in 18 mL of buffer C overnight at 4 °C and then burst by incubation for 45 min at 37 °C after addition of Pronase (0.5 mg/mL) and SDS (2% w/v) to the solution. The lysate was extracted 3 times with freshly distilled phenol. Residual phenol was removed by multiple extractions with ether. The DNA was precipitated by adding 0.1 volume of 3 M NaCl and 2 volumes of ethanol. The pellet was carefully washed to remove excess salt, gently dried, and stored at −20 °C. A yield of 2.15 mg of DNA was obtained from 18 mg of virus (theoretical DNA content = 2.7 mg). Agarose gel electrophoresis of this DNA preparation showed a single band migrating as terminal-protein-free PRD1 DNA.

Raman Spectroscopy. Stock solutions of PRD1 phage and PRD1 capsomers (P3 protein), prepared in the Helsinki laboratory, were further concentrated for Raman spectroscopy at the University of Missouri—Kansas City laboratory using the following procedures. For PRD1 phage, 200-μL aliquots of the stock solution (containing 1.5 mg of phage/mL in buffer C) were pelleted at 4 °C by centrifugation for 8 min at 160000*g* in a Beckman Airfuge (A-100/30 rotor). The pellets were pooled to yield approximately 30 μL of PRD1 concentrate, from which Raman spectra were recorded. Similar procedures were used for both 1× and 2× purified virus. At the resolution employed in this work, no significant Raman spectral differences could be detected between 1× and 2× products.

For P3, 400-μL aliquots of the stock solution (containing 0.1 mg/mL in buffer C) were introduced into a Millipore Ultrafree-MC concentrator and subjected to centrifugal sieving through a 10-kDa filter by spinning at 8000 rpm for 24 min in an Eppendorf Model-5415 centrifuge. The retentates were pooled to yield 40 μL of concentrated P3 solution. All ultrafiltrations were carried out at 4 °C using filters which had been prewashed successively with 1% NaOH, deionized H_2O, and buffer C.

Approximately 10-μL aliquots of the concentrated phage (PRD1) and protein (P3) solutions were loaded into Raman sample cells (Kimax 34507 capillary tubes) and sealed. The intensities of Raman signals obtained from these samples indicated that solute concentrations were approximately 100 μg/μL for PRD1 and 50 μg/μL for P3.

Lyophilized PRD1 DNA (Helsinki) was reconstituted for Raman spectroscopy in deionized water to a final concentration of 40 μg/μL at pH 7.07. Aliquots of the DNA solution were loaded into cells and sealed for Raman spectroscopy.

The sealed capillaries were mounted in a precision thermostat for Raman spectroscopic analysis (Thomas & Barylski, 1970). Raman spectra were collected from phage samples thermostated at 4 °C and from P3 and DNA samples thermostated at 20 °C. All data were collected within 150 h of the time of preparation of the concentrated or reconstituted samples, during which time no sample degradation could be detected. Previous studies indicate that viral infectivity, as measured by the number of plaque forming units, is not diminished by more than 10% for every 100 h of storage at these conditions.

Raman spectra were excited with the 514.5-nm line from an argon ion laser (Coherent Innova 70-2) using approximately 200 mW of radiant power at the sample. Raman scattering at 90° to the incident laser beam was collected and analyzed with a Spex Ramalog V/VI spectrometer (Li et al., 1981), operating under the control of an IBM-PC. Programs for instrument control and data collection were developed in our

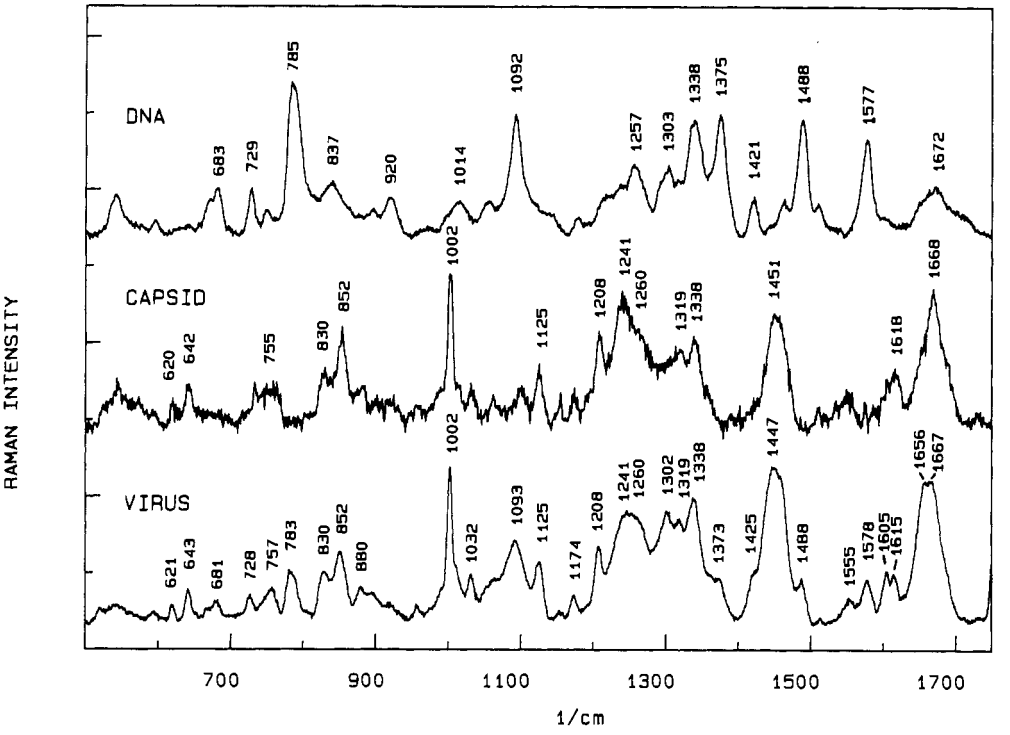

FIGURE 1: Raman spectra in the region 500–1750 cm^{-1} of PRD1 virus (bottom), PRD1 capsid protein P3 (middle), and PRD1 DNA (top).

laboratory using the ASYST language (Asyst Software Technologies). A detailed description of this software implementation will be given elsewhere (B. Prescott and G. J. Thomas, Jr., unpublished results).

Data were collected with a spectral slit width of 8 cm^{-1}, at increments of 1 cm^{-1} and with an integration time of 1.5 s. Spectra of the three samples were collected in the region 500–1750 cm^{-1}, and the Raman intensities from 16, 4, and 4 consecutive scans, respectively, of PRD1, P3, and DNA were averaged for presentation below. Additionally, spectra of superior signal-to-noise in the 600–950 cm^{-1} region of PRD1 DNA were obtained by accumulating up to 15 scans. The Raman intensity data were corrected for scattering by the buffer, and for the gently sloping background characteristic of aqueous solution spectra of viruses and viral components (Verduin et al., 1984). The scattering background was found to improve significantly for both intact phage and P3 samples after a few minutes of exposure to the low-intensity laser beam. This effect has been attributed to quenching of low-intensity fluorescence from dissolved oxygen molecules in the aqueous sample (M. Tsuboi, private communication). Signal averaging, base-line corrections, spectral subtractions, and related data manipulations were performed through ASYST routines.

Results and Discussion

Figure 1 shows Raman spectra in the region 500–1750 cm^{-1} of PRD1 (virus), P3 capsomers (capsid), and isolated PRD1 DNA. The isolated DNA is a double-stranded linear molecule of about 14 700 base pairs and is expected to assume a classical B-DNA conformation in solution at the conditions investigated. This is confirmed by the spectrum of Figure 1 (top trace) which exhibits all of the characteristic Raman bands of B-DNA (Erfurth et al., 1972; Prescott et al., 1984; Thomas et al., 1986). The most prominent Raman bands of B-DNA also appear without noticeable change in the Figure 1 spectrum of the virus (bottom trace), which indicates that the packaged viral DNA retains the B-form secondary structure. The B-DNA markers are labeled in the spectrum of Figure 1 and are included in the tabulation of Raman bands of the virus (Table I). The 600–900 cm^{-1} region of the PRD1 DNA spectrum is shown in Figure 2 on an expanded scale to illustrate specific nucleoside and backbone conformation markers of the B form (Thomas & Wang, 1988). Figure 2 also compares the PRD1 Raman profile in this region with that of another dsDNA of rather similar base composition (45% GC), the replicative-form DNA (RFII DNA) of bacteriophage ϕX174 (Sanger et al., 1978). Further discussion of Figure 2 is given under Conclusions.

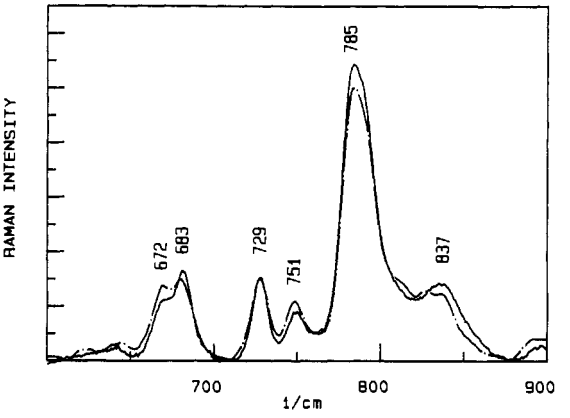

FIGURE 2: Raman spectrum of PRD1 DNA (—) compared with that of the double-stranded replicative form (RFII) of ϕX174 DNA (–·–). ϕX174 DNA was a gift from Prof. N. Incardona, University of Tennessee—Memphis.

The Figure 1 spectrum of the capsomers (middle trace) is dominated by strong and relatively sharp amide I and amide III bands at 1668 and 1241 cm^{-1}, respectively. These markers clearly identify the β-sheet as the predominant secondary structure in P3 subunits (Chen & Lord, 1974; Sargent et al., 1988). The weak amide III shoulder near 1250–1260 cm^{-1} indicates a contribution also from irregular domains of the P3 subunits. Although the present data exhibit appreciable background noise and do not warrant a detailed quantitative description, it is estimated from comparison with Raman spectra of other viral proteins (Thomas et al., 1982; Sargent

Table I

Raman frequency (intensity)[a]	assignment[b]
543 (w)	ade, sc
595 (w)	gua, cyt, sc
621 (w)	F
643 (w)	Y
681 (w)	gua
728 (w)	ade
751 (w, S)	thy
757 (m)	W
783 (m)	cyt
790 (m, S)	bk, phos
830 (m)	Y, bk
852 (m)	Y
880 (m)	W, ac [CC str]
896 (w)	bk, ac [CC str]
920 (w)	bk, ac [CC str], sc
958 (w)	sc [CH def], PL
991 (w, S)	sc
1002 (s)	F
1011 (m, S)	W, bk
1032 (m)	F, bk
1066 (m, B, S)[c]	ac [CC str], bk, sc
1093 (m, B)[c]	bk, phos
1125 (m)	sc [CC,Cn str], ac [CC str]
1155 (w)	sc [CH def]
1174 (w)	sc [CH def]
1208 (m)	Y, F
1241 (s, B)	AmIII
1260 (s, B, S)	AmIII, cyt
1302 (s)	AmIII, sc [CH def], ac [CH def], ade
1319 (s)	AmIII, sc [CH def], gua
1338 (s)	sc [CH def], W, ade, gua
1373 (m, S)	thy, gua
1425 (m, S)	sc [CH def], ade, gua
1447 (s, B)	ac [CH def]
1457 (s, S)	sc [CH def]
1488 (m)	gua, ade
1555 (w)	W
1578 (m)	gua, ade, W
1605 (m)	F
1615 (m)	Y, cyt
1656 (s, S)	PL
1667 (s, B)	AmI, gua, thy, cyt

[a] Raman frequencies in cm^{-1} units are accurate to ± 2 cm^{-1}. Abbreviations: w, weak; m, medium; s, strong; S, unresolved shoulder; B, broad band. [b] Abbreviations for DNA groups: ade, adenine; gua, guanine; thy, thymine; cyt, cytosine; bk, backbone. Protein groups: AmI, amide I; AmIII, amide III; F, phenylalanine; W, tryptophan; Y, tyrosine; sc, side chains. Phospholipid (PL) groups: phos, phosphate head group; ac, acyl side chains. Where possible, detailed assignments are enclosed in brackets, with CC, CN, and CH indicating specific chemical groups of protein or lipid side chains, and str and def indicate stretching and deformation modes, respectively. [c] The broad 1066 cm^{-1} shoulder to the 1093 cm^{-1} band encompasses the lipid liquid-crystalline phase marker (1078 cm^{-1}, see Figure 3) and lesser contribution from DNA and protein (Figure 1).

et al., 1988; Li et al., 1990) that the P3 subunit contains about 40–60% β-sheet secondary structure.

Among other prominent Raman bands of the capsomers, the tryptophan band at 1339 cm^{-1} and the tyrosine bands at 829 and 854 cm^{-1} are most easily correlated with protein side chain interactions (Miura et al., 1988; Siamwiza et al., 1975). Accordingly, the data of Figure 1 indicate that, on average, the tryptophan residues of P3 are in a hydrophilic environment. This determination is based upon the appearance of the strong tryptophan band at 1339 cm^{-1} and the absence of a companion band at 1360 cm^{-1} (Harada et al., 1986; Miura et al., 1988). [We regard the weak tryptophan band near 882 cm^{-1} in the P3 spectrum as inconclusive with regard to indole hydrogen bonding because of the relatively high noise level in this spectrum; see Miura et al. (1988).] The P3 data also indicate that, on average, the phenolic OH groups of tyrosine residues act as both donors and acceptors of moderately strong hydrogen bonds, although the acceptor role is more prevalent. This conclusion is based upon the measured ratio of Raman intensities of tyrosine bands at 854 and 829 cm^{-1}, for which $I_{854}/I_{829} = 1.8$ (Siamwiza et al., 1975).

The Raman spectrum of the intact phage (Figure 1, bottom trace) represents a complex molecular assembly of protein, DNA, and lipid. All of the prominent bands of PRD1 DNA and P3 are recognizable in the spectrum of the virus. This indicates that no major structural changes occur in either DNA or P3 upon DNA packaging. The virus also exhibits a number of bands not present in spectra of either the DNA or the P3 molecules. These are attributed to the viral membrane and are identified as Raman bands of the membrane lipid in Table I. The lipid assignments in Table I are supported by the fact that corresponding bands are observed in Raman spectra of purified phospholipids and lipoprotein vesicles (Lord & Mendelsohn, 1981; Levin, 1984). In further support of these assignments, we note that the nonlipid (i.e., protein) composition of the viral membrane represents less than 20% of the total protein in the virion and is expected to contribute only very weakly to the Raman spectrum (Davis et al., 1982).

An improved visualization of the contribution of the viral membrane to the Raman spectrum of the virus can be obtained by subtracting the spectra of DNA and of capsomer from the virus spectrum. For this subtraction, the DNA contribution is scaled to fully compensate the strong DNA bands at 783 and 790 cm^{-1} (Table I), while the capsomer contribution is scaled to fully compensate the strong and sharp band of phenylalanine at 1002 cm^{-1}. The Raman spectrum of the viral membrane generated in this manner using digital subtraction methods is shown in the bottom trace of Figure 3. This approach assumes that (i) Raman bands of the minor capsid proteins and membrane-embedded proteins (altogether about 20% of the total viral protein) do not on average differ greatly from those of P3 capsomers and that (ii) the lesser proteins do not contribute greatly to the Raman spectrum in those regions where lipid bands are most prominent. Both of these assumptions are reasonable in the context of the present analysis (Lord & Mendelsohn, 1981; Spiro, 1987). The membrane spectrum generated in Figure 3 allows the tentative conclusion that lipids of the viral membrane are in a liquid-crystalline phase, rather than in a gel-like phase at the experimental conditions employed. Specifically, the strong bands at 1078, 1301, and 1440 cm^{-1} and the weak bands at 1068 and 1128 cm^{-1} are characteristic of Raman spectra of many membrane phospholipids in the liquid-crystalline state (Lord & Mendelsohn, 1981; Levin, 1984). We note that the 1078 cm^{-1} frequency is unambiguously assigned to lipid, since neither the DNA nor the protein yields comparable Raman intensity at this frequency. In agreement with a liquid-crystalline lipid phase is the absence of intense Raman markers at 1060 and 1130 cm^{-1} which are diagnostic of the lipid gel phase (Lord & Mendelsohn, 1981; Levin, 1984). We stress that this is a preliminary conclusion which will require further corroboration by a spectrum of the viral membrane exhibiting superior signal-to-noise quality to that generated in Figure 3.

Direct measurement of phase transitions in PRD1-type phage lipids has not been reported previously, although the effect of lipid composition on phase transitions has been discussed and indications of liquid-crystalline lipids have been speculated (Muller & Cronan, 1983). The present results directly demonstrate the liquid-crystalline lipid state in the PRD1 membrane. We are currently working toward obtaining sufficient quantities of empty virus particles and soluble viral

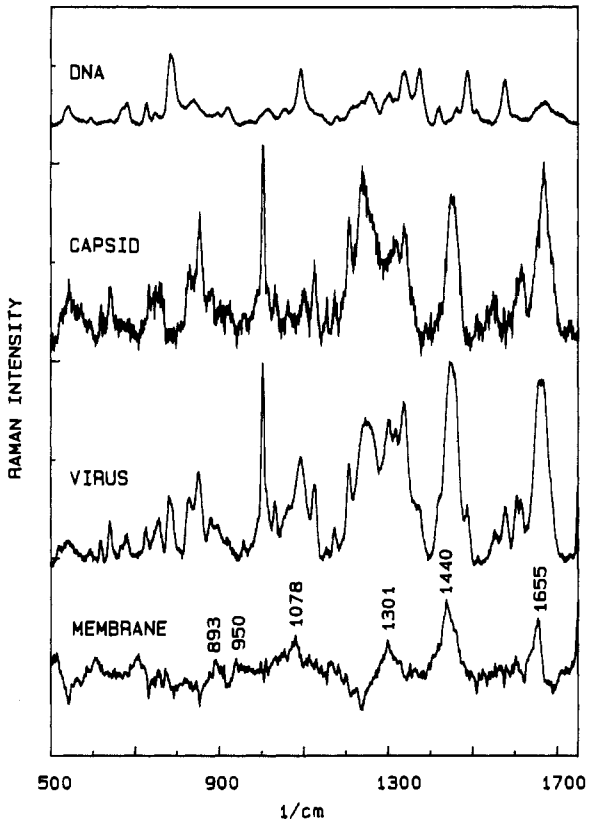

FIGURE 3: Computed Raman spectrum of the membrane of PRD1 (bottom) obtained by subtraction of the sum of spectra observed for DNA (top) and capsid (second from top) from the spectrum observed for the intact virion (second from bottom). In this illustration, spectra of viral components (DNA and capsomer) are scaled to match their corresponding intensities (783–790 and 1002 cm^{-1}) in the virion spectrum (see Table I).

membranes to conduct more detailed experimental studies of their phase transitions.

Conclusions

We have obtained the first Raman vibrational spectrum of a membrane-containing virus, the bacteriophage PRD1, and demonstrated the appearance in the spectrum of structure markers from viral protein, DNA, and lipid. We have also demonstrated use of the Raman markers to infer structural properties of each of the three classes of biomolecular components in the virion. The method of digital difference Raman spectroscopy has provided a first approximation to the structure of the phospholipid in the viral membrane, indicating a liquid-crystalline lipid phase. This preliminary finding was not predictable because many model phospholipid bilayers and vesicles exist in the gel phase at the temperature (4 °C) employed in the present investigation (Lord & Mendelsohn, 1981; Levin, 1984).

Our results show that the major capsid protein of PRD1 is predominantly in the β-strand conformation, which is in accord with results obtained from other icosahedral bacteriophages and eukaryotic viruses (Thomas, 1987; Thomas et al., 1982; Rossman & Johnson, 1989). We have also inferred from the present results that the viral membrane, which encloses the dsDNA genome, does not greatly perturb the B-form secondary structure of PRD1 DNA. The structure of the packaged viral chromosome of PRD1 does not appear to differ significantly from the condensed genomes of bacteriophages P22 and T7 (G. J. Thomas, Jr., J. King, and P. Serwer, unpublished results), although the latter lack a membrane lining to the capsid wall. This conclusion will require further confirmation by direct measurement of spectra of the viral membrane extracted from PRD1. Such work is currently in progress.

Finally, we note from Figure 2 that the naked dsDNA of ϕX174, which contains approximately 8% less GC and 8% more AT than PRD1 DNA, exhibits the anticipated 8% lower Raman intensity for bands assigned to G (683 cm^{-1}) and C (785 cm^{-1}) and correspondingly higher intensities for bands of T (672 and 751 cm^{-1}). Surprisingly, however, the two DNAs do not exhibit a significant intensity difference in the band of A at 729 cm^{-1}, presumably a result of compensating effects associated with the different base sequences. We also note that the broad band centered near 837 cm^{-1} differs somewhat in shape and relative intensity in these two DNAs, reflecting subtle differences in backbone geometry which may be associated with differences in the organization of linear PRD1 DNA and circular RFII ϕX174 DNA.

Since the lipid moiety of *E. coli* bacteriophage PRD1 can be probed within the virion by Raman spectroscopy, we have demonstrated a practical approach to investigating the membrane of enveloped viruses in situ. This approach may also provide a convenient means of modeling other membrane bilayer–protein assemblies.

Acknowledgments

We thank Dr. J. M. Benevides for assistance in data collection and discussions. We also thank Dr. N. Incardona, University of Tennessee—Memphis, for providing dsDNA from bacteriophage ϕX174.

References

Bamford, D. H., & Mindich, L. (1982) *J. Virol. 44*, 1031–1038.
Bamford, D. H., & Mindich, L. (1984) *J. Virol. 50*, 309–331.
Bamford, D. H., Rouhiainen, L., Takkinen, K., & Soderlund, H. (1981) *J. Gen. Virol. 57*, 365–373.
Bamford, J. K. H., & Bamford, D. H. (1990) *Virology* (in press).
Bradford, M. M. (1976) *Anal. Biochem. 72*, 248–254.
Carey, P. R. (1982) *Biochemical Applications of Raman and Resonance Raman Spectroscopies*, Academic Press, New York.
Chen, M. C., & Lord, R. C. (1974) *J. Am. Chem. Soc. 96*, 4750–4752.
Davis, T. N., & Cronan, J. E., Jr. (1983) *Virology 126*, 600–613.
Davis, T. N., & Cronan, J. E., Jr. (1985) *J. Biol. Chem. 260*, 663–671.
Davis, T. N., Muller, E. D., & Cronan, J. E., Jr. (1982) *Virology 120*, 287–306.
Erfurth, S. C., Kiser, E. J., & Peticolas, W. L. (1972) *Proc. Natl. Acad. Sci. U.S.A. 69*, 938–941.
Harada, I., Miura, T., & Takeuchi, H. (1986) *Spectrochim. Acta 42A*, 307–312.
Levin, I. W. (1984) *Adv. Infrared Raman Spectrosc. 2*, 1–48.
Li, Y., Thomas, G. J., Jr., Fuller, M., & King, J. (1981) *Prog. Clin. Biol. Res. 64*, 271–283.
Li, T., Chen, Z., Johnson, J. E., & Thomas, G. J., Jr. (1990) *Biochemistry 29*, 5018–5026.
Lord, R. C., & Mendelsohn, R. (1981) *Mol. Biol. Biochem. Biophys. 31*, 377–436.
Maniatis, T., Fritsch, E. F., & Sambrook, J. (1982) *Molecular Cloning: A Laboratory Manual*, Cold Spring Harbor Press, Cold Spring Harbor, NY.
McGraw, T., Yang, H., & Mindich, L. (1983) *Mol. Gen. Genet. 190*, 237–244.

Mindich, L., & Bamford, D. H. (1988) in *The Bacteriophages* (Calendar, R., Ed.) Vol. 2, pp 475–520, Plenum Press, New York.
Mindich, L., Bamford, D., McGraw, T., & Mackenzie, G. (1982a) *J. Virol. 44*, 1021–1030.
Mindich, L., Bamford, D., Goldthwaite, C., Laverty, M., & Mackenzie, G. (1982b) *J. Virol. 44*, 1013–1020.
Miura, T., Takeuchi, H., & Harada, I. (1988) *Biochemistry 27*, 88–94.
Muller, E. D., & Cronan, J. E., Jr. (1983) *J. Mol. Biol. 165*, 109–124.
Olsen, R. H., Siak, J., & Gray, R. H. (1974) *J. Virol. 14*, 689–699.
Prescott, B., Steinmetz, W., & Thomas, G. J., Jr. (1984) *Biopolymers 23*, 235–256.
Rossman, M. G., & Johnson, J. E. (1989) *Annu. Rev. Biochem. 58*, 533–573.
Saier, M. H., Jr., Werner, P. K., & Muller, M. (1989) *Microbiol. Rev. 53*, 333–366.
Salas, M. (1988) in *The Bacteriophages* (Calendar, R., Ed.) Vol. 1, pp 169–186, Plenum Press, New York.
Sanger, F., Coulson, A. R., Freidmann, T., Air, G. M., Barrell, B. G., Brown, N. L., Fiddes, J. C., Hutchison, C. A., III, Slocombe, P. M., & Smith, M. (1978) *J. Mol. Biol. 125*, 225–246.
Sargent, D., Benevides, J. M., Yu, M.-H., King, J., & Thomas, G. J., Jr. (1988) *J. Mol. Biol. 199*, 491–502.
Savilahti, H., & Bamford, D. H. (1986) *Gene 49*, 199–205.
Siamwiza, M. N., Lord, R. C., Chen, M. C., Takamatsu, T., Harada, I., Matsuura, H., & Shimanouchi, T. (1975) *Biochemistry 14*, 4870–4876.
Spiro, T. G., Ed. (1987) *Biological Applications of Raman Spectroscopy*, Vol. 1, Wiley-Interscience, New York.
Tamanoi, F. (1986) in *Adenovirus DNA* (Doerfler, W., Ed.) pp 97–128, Martinus Nijhoff, Boston, MA.
Thomas, G. J., Jr. (1987) in *Biological Applications of Raman Spectroscopy* (Spiro, T. G., Ed.) Vol. 1, pp 135–201, Wiley-Interscience, New York.
Thomas, G. J., Jr., & Barylski, J. (1970) *Appl. Spectrosc. 24*, 463–464.
Thomas, G. J., Jr., & Kyogoku, Y. (1977) *Pract. Spectrosc. 1C*, 717–872.
Thomas, G. J., Jr., & Wang, A. H.-J. (1988) *Nucleic Acids Mol. Biol 2*, 1–30.
Thomas, C. J., Jr., Li, Y., Fuller, M. T., & King, J. (1982) *Biochemistry 21*, 3866–3878.
Thomas, G. J., Jr., Benevides, J. M., & Prescott, B. (1986) *Biomol. Stereodyn. 4*, 227–253.
Tu, A. T. (1986) in *Spectroscopy of Biological Systems* (R. J. H. & Hester, R. E., Eds.) pp 47–112, Wiley, New York.
Verduin, B. J. M., Prescott, B., & Thomas, G. J., Jr. (1984) *Biochemistry 23*, 4301–4308.
Wong, F. H., & Bryan, L. E. (1978) *Can. J. Microbiol. 24*, 875–882.

Structural Studies on the Active Site of *Escherichia coli* RNA Polymerase. 1. Interaction of Metals on the *i* and *i* + 1 Sites

Peter P. Chuknyisky, Joseph M. Rifkind, Edward Tarien, Richard B. Beal, and Gunther L. Eichhorn*
National Institutes of Health, National Institute on Aging, Gerontology Research Center, Laboratory of Cellular & Molecular Biology, Baltimore, Maryland 21224

Received November 28, 1989; Revised Manuscript Received March 20, 1990

ABSTRACT: The two substrates between which an internucleotide bond is formed in RNA synthesis occupy two subsites, *i* and *i* + 1, on the active site of *Escherichia coli* RNA polymerase, and each subsite is associated with a metal ion. These ions are therefore useful as probes of substrate interaction during RNA synthesis. We have studied interactions between the metals by EPR spectroscopy. The Zn(II) in the *i* site and the Mg(II) in the *i* + 1 site were substituted separately or jointly by Mn(II). The proximity of the metals was established by EPR monitoring of the titration at 5.5 K of the enzyme containing Mn(II) in *i* with Mn(II) going into the *i* + 1 site, and the 1:1 ratio of the metals in the two sites was confirmed in this way. The distance between the two metals was determined by EPR titration at room temperature of both the enzyme containing Zn(II) in *i* and Mn(II) in *i* with Mn(II) going into the *i* + 1 site, making use of the fact that EPR spectra are affected by dipolar interactions between the metals. The distances calculated in the presence of enzyme alone, in the presence of enzyme and two ATP substrates, and when poly(dAdT)·poly(dAdT) was added to the latter system ranged from 5.2 to 6.7 Å.

The regulation of RNA synthesis is one of the most important processes in molecular biology, and its mechanism involves a variety of components, many of which are concerned with initiation and termination. We shall concern ourselves with the possibility that regulation can occur at the point of bond formation and have begun a series of investigations to determine whether the geometry of interaction at that point can change in a way that can have regulatory significance.

The synthesis of RNA is mediated by the enzyme RNA polymerase, which in *Escherichia coli* has a molecular mass of $\sim^1/_2$ million daltons, and consists of five subunits (two α, β, and β' for core enzyme, plus σ factor in holoenzyme). This enzyme is involved in a variety of functions required in the regulation of RNA synthesis, but its central function is to bring together two substrates for the purpose of forming an internucleotide bond between them. In this central process of RNA synthesis the oxygen atom at the 3′ terminus of the growing RNA chain reacts with the α-phosphorus of a nucleoside triphosphate (NTP) to form a phosphodiester bond, with the concomitant loss of pyrophosphate.